NASA TECHNICAL NOTE

NASA TN D-2475

ANALYTICAL STUDY OF THE EXPANSION AND CONDENSATION BEHAVIOR OF ALKALI-METAL AND MERCURY VAPORS FLOWING THROUGH NOZZLES

by Arthur J. Glassman

Lewis Research Center
Cleveland, Ohio

NATIONAL AERONAUTICS AND SPACE ADMINISTRATION • WASHINGTON, D. C. • SEPTEMBER 1964

ANALYTICAL STUDY OF THE EXPANSION AND CONDENSATION BEHAVIOR OF ALKALI-METAL AND MERCURY VAPORS FLOWING THROUGH NOZZLES

By Arthur J. Glassman

Lewis Research Center
Cleveland, Ohio

NATIONAL AERONAUTICS AND SPACE ADMINISTRATION

For sale by the Office of Technical Services, Department of Commerce,
Washington, D.C. 20230 -- Price $0.75

ANALYTICAL STUDY OF THE EXPANSION AND CONDENSATION BEHAVIOR OF ALKALI-METAL AND MERCURY VAPORS FLOWING THROUGH NOZZLES

by Arthur J. Glassman

Lewis Research Center

SUMMARY

This investigation was undertaken in order to gain some insight to the expansion and condensation behavior of alkali-metal and mercury vapors flowing through nozzles. A comparison of the equilibrium with the frozen mode of expansion showed that different expansion mode assumptions can result in significant differences in the computed values of such important turbine design parameters as ideal specific enthalpy drop and flow area per unit weight flow. Nucleation rates were then examined and condensation theory, such as that used successfully to predict the condensation behavior of steam during rapid expansion, was applied to the flow of metal vapors in nozzles. Sodium, potassium, rubidium, cesium, and mercury were investigated at nozzle inlet temperatures of 1700° to 2500° R for the alkali metals and 1200° to 1600° R for mercury.

Mercury was found to expand to quite low pressure ratios (exit to inlet) without condensing. The alkali metals condense upstream of the nozzle throat for all cases investigated with the exception of sodium at nozzle inlet temperatures below about 1950° R. Increasing either nozzle inlet temperature or alkali-metal molecular weight results in the condensation point moving towards the nozzle inlet. A large increase in expansion time results in only a very small increase in the pressure ratio at which condensation occurs. The use of superheat can significantly delay the condensation. The uncertainties inherent in the available surface tension values can significantly affect the location of the calculated condensation point.

A simplified estimation procedure was evolved for predicting the location of the condensation point on the basis of a nucleation rate criterion. The more rigorous nozzle analysis showed that this estimation procedure yielded reasonable approximations.

INTRODUCTION

Electric power production in outer space is one of the critical require-

ments for the fulfillment of a great many of the objectives of space exploration. The most promising power-generation technique for near-future application to missions requiring power levels in excess of several kilowatts for extended periods of time appears to be the indirect-conversion closed-loop heat engine. Such a system utilizes the conversion of nuclear or solar heat to mechanical shaft power, which, in turn, is converted to electrical power. One of the thermodynamic cycles most often considered for such a system is the Rankine cycle. For space application, a metal working fluid is used because of the high temperature levels dictated by heat rejection considerations.

One of the major components of a Rankine cycle power system is the turbine, which serves to expand the fluid to a high velocity and convert fluid kinetic energy to mechanical shaft power. The proper design of a turbine depends upon a knowledge of the fluid state during and after the expansion process in order to evaluate correctly the energy available to do work and the required flow areas. When a saturated vapor expands through a nozzle, the expansion and condensation processes do not follow the usual vapor-liquid equilibrium relations. A certain amount of supersaturation (undercooling of a vapor below its saturation temperature without condensation) occurs, the amount depending upon the nature of the fluid, its initial state, and the degree and rapidity of the expansion. The expansion process for alkali metal vapors is further complicated by the existence of monomer, dimer, and possibly other polymeric species in the vapor phase. The equilibrium concentrations of the species have been determined only theoretically and the dimerization reaction rates are unknown; the state of the fluid during expansion and the point of condensation, consequently, are neither readily nor accurately predictable. In view of these considerations, turbine design procedures, for purposes of convenience, have been based upon the assumption of one of the pure modes (equilibrium or frozen) of expansion.

In view of the many uncertainties associated with the expansion of metal vapors, an attempt was made to gain some insight to the behavior of these fluids by studying analytically certain aspects of the expansion process. The equilibrium and frozen modes of expansion were first compared in order to determine the significance of the expansion mode assumption with regard to ideal enthalpy drop and flow area. A condensation analysis was then carried out in order to gain some insight to the true expansion mode. An analysis somewhat similar to the one being reported herein was made in reference 1 and applied to a few isolated cases. This report presents parametric results that cover the full range of interest for both fluid and temperature, as well as the effects of expansion time, superheat, and surface tension. Sodium, potassium, rubidium, cesium, and mercury were investigated at nozzle inlet saturation temperatures of 1700° to 2500° R for the alkali metals and 1200° to 1600° R for mercury.

SYMBOLS

A flow area, sq ft

c_p frozen specific heat, Btu/(lb)(°R)

g	gravitational constant, 32.2 $(ft)(lb_{mass})/(sec^2)(lb_{force})$
h	specific enthalpy, Btu/lb
Δh	specific enthalpy drop, Btu/lb
I^*	nucleation rate, nuclei, sec^{-1} ft^{-3}
J	mechanical equivalent of heat, 778 (ft)(lb)/Btu
k	Boltzmann gas constant, 5.652 (10^{-24})(ft)(lb)/^oR
M	molecular weight, lb/lb mol
N	Avogadro number, 2.732 (10^{26})(molecules)/lb mol
p	absolute pressure, lb/sq ft
q	vapor quality, weight fraction
R	universal gas constant, 1544 (ft)(lb)/(lb mol)(^oR)
r	radius of drop, ft
$r_{x',x}$	radius at x of drop formed at x', ft
r^*	radius of condensation nucleus, ft
s	specific entropy, Btu/(lb)(^oR)
T	absolute temperature, ^oR
u	velocity, ft/sec
w	weight flow, lb/sec
x,x'	distance along nozzle, ft
γ	frozen specific heat ratio
λ	parameter defined by equation (10)
ρ	density, lb/cu ft
σ	surface tension, lb/ft

Subscripts:

c	critical
E	equilibrium

F	frozen
l	liquid
mp	melting point
o	initial
s	saturation
V	vaporization
v	vapor
x,x'	position x or x'

COMPARISON OF EXPANSION MODES

As pointed out in the INTRODUCTION, the existence of supersaturation and dimerization in the vapor phase complicate the expansion process, and the fluid properties during and after expansion cannot be determined readily. Turbine design procedures, consequently, have been based on the assumption of a particular expansion mode in order to compute the parameters, such as ideal specific enthalpy drop and area per unit weight flow, hereinafter referred to as specific area, that are necessary for proper sizing of the turbine. The usually assumed expansion modes are those for which the necessary computations can be readily made; that is, either equilibrium or frozen with respect to both the moisture and molecular specie contents throughout a nozzle. The computed values for ideal specific enthalpy drop and specific area will, of course, differ according to the imposed assumption.

In order to determine the extent of the differences caused by the expansion mode assumption, ideal specific enthalpy drop and specific area for equilibrium and frozen expansions with sodium, potassium, rubidium, and cesium were machine computed and compared. For any given inlet condition and pressure ratio, the data of reference 2 was used to obtain the final temperatures, final vapor qualities, ideal specific enthalpy drops, and specific areas for both equilibrium and frozen isentropic expansions. For an equilibrium expansion, the final temperature was obtained from the given vapor pressure equation, while the initial and final enthalpies and entropies were obtained from the tabulated thermodynamic data. Since the process is isentropic, the final quality was determined from

$$s_x = s_o = q_{x,E} s_{v,x,E} + (1 - q_{x,E}) s_{l,x,E}$$

and the ideal specific enthalpy drop was then determined from

$$\Delta h_E = h_o - h_{x,E} = h_o - q_{x,E} h_{v,x,E} - (1 - q_{x,E}) h_{l,x,E}$$

Position x in the nozzle is the point corresponding to the final conditions of the expansion. For a frozen expansion, the final vapor quality is equal to unity, and the perfect gas laws are used to compute the desired final temperature and enthalpy drop as follows:

$$T_{x,F} = T_o\left(\frac{p_x}{p_o}\right)^{\frac{\gamma_o - 1}{\gamma_o}}$$

and

$$\Delta h_F = c_{p,o}(T_o - T_{x,F})$$

Specific areas for both expansions were then obtained from the continuity equation

$$\frac{A_x}{w} = \frac{1}{\rho_x u_x}$$

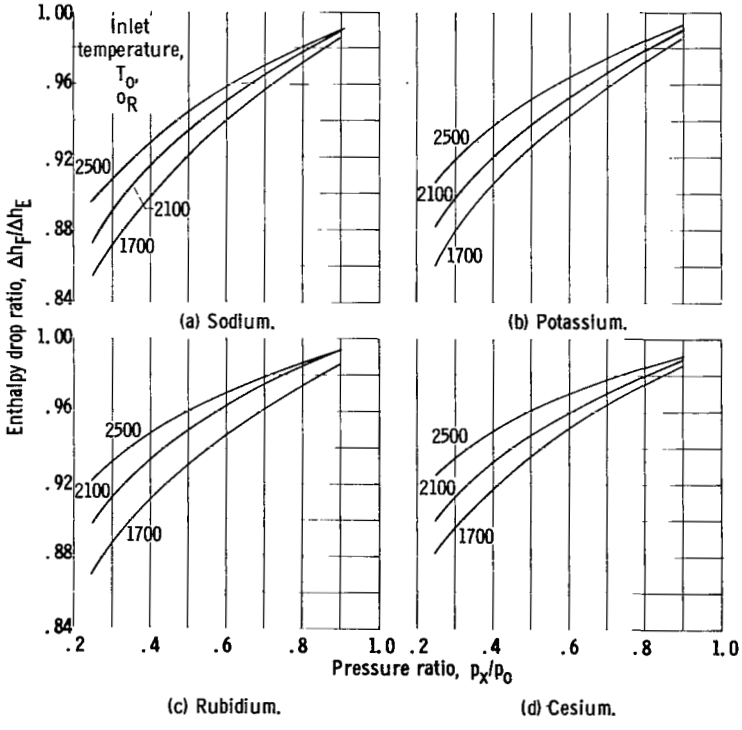

Figure 1. - Comparison of frozen and equilibrium ideal specific enthalpy drop.

where

$$u_x = \sqrt{2gJ\,\Delta h}$$

and

$$\rho_x = \frac{1}{\frac{q_x}{\rho_{v,x}} + \frac{1 - q_x}{\rho_{l,x}}}$$

The vapor density ρ_v was obtained from the perfect gas law

$$\rho_{v,x} = \frac{p_x M_x}{R T_x}$$

For a frozen expansion, $q_x = 1$ and $M_x = M_o$. All the required properties were obtained from reference 2. The results of the ideal specific enthalpy drop and the specific area comparisons are presented in figures 1 and 2, respectively. The vapors were assumed to be saturated at the nozzle inlet.

The ratio of frozen to equilibrium ideal specific enthalpy drop $\Delta h_F/\Delta h_E$ is presented in figure 1 as a function of expansion pressure ratio (ratio of final to initial pressure) for sodium, potassium, rubidium, and cesium with inlet temperatures of 1700°, 2100°, and 2500° R. For any given pressure ratio, a frozen expansion yields less ideal specific enthalpy drop than an equilibrium expansion. The difference between frozen and equilibrium ideal specific enthalpy drop increases (decreasing enthalpy drop ratio) with increasing degree of expansion (decreasing pressure ratio) and decreasing inlet temperature. For the range of variables considered herein, the maximum difference between frozen and equilibrium ideal specific enthalpy drop is about 12 to 15 percent. For a pressure ratio of 0.5, which approximately corresponds to a choked convergent nozzle, frozen enthalpy drop is about 4 to 8 percent less than equilibrium enthalpy drop.

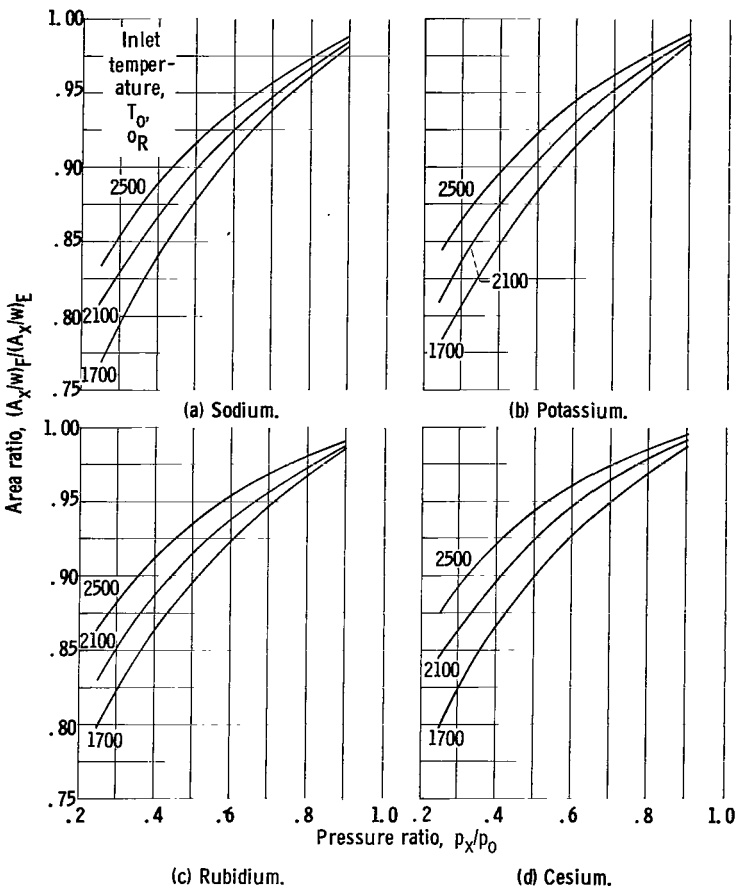

Figure 2. - Comparison of frozen and equilibrium specific flow area.

The ratio of frozen to equilibrium specific area is presented in figure 2 as a function of expansion pressure ratio for sodium, potassium, rubidium, and cesium with inlet temperatures of 1700°, 2100°, and 2500° R. For any given pressure ratio, less area is required for a given weight flow when the expansion is frozen than when it is in equilibrium. Although the frozen velocity is less than the equilibrium velocity because of the lower ideal specific enthalpy drop, the increased density resulting from the lower temperature of the frozen flow accounts for the lower specific area. The difference between frozen and equilibrium specific area increases (decreasing area ratio) with increasing degree of expansion (decreasing pressure ratio) and decreasing inlet temperature. For the range of variables considered herein the maximum difference between frozen and equilibrium specific area is about 20 to 24 percent. For a pressure ratio of 0.5, which approximately corresponds to the throat of a sonic or supersonic nozzle, frozen specific area is about 6 to 12 percent less than equilibrium specific area.

There is one further point that may be of interest as far as the comparison of frozen to equilibrium expansion is concerned. A common method used in

steam turbine design practice for correlating the energy loss due to supersaturation has been in terms of the ratio of the fraction of equilibrium energy lost $1 - \frac{(\Delta h_F)}{(\Delta h_E)}$ to the fractional moisture content $1 - q_{x,E}$ that would accompany an equilibrium expansion. Such a factor was used for the few example metal vapor cases studied in reference 1. Such a correlation allows the use of equilibrium charts as a design tool for cases where supersaturation is known to exist. The ratio of energy loss to moisture is plotted against inlet temperature in figure 3 for sodium, potassium, rubidium, and cesium. For the range of pressure ratios (0.25 to 0.9) considered herein, the loss to moisture ratio within the precision inherent in this computation showed no significant trend that could be attributed to the effect of pressure ratio. At an inlet temperature of 1700° R, the loss to moisture ratio is about 1.18 for rubidium and cesium, 1.43 for potassium, and 1.67 for sodium. An increase in inlet temperature from 1700° to 2500° R results in about a 50-percent reduction in loss to moisture ratio.

The foregoing discussion has shown that different expansion mode assumptions can result in significant differences in the computed values of such important turbine design parameters as ideal specific work and specific area. Further study of the expansion and condensation behavior of metal vapors flowing through nozzles, therefore, is desirable in order to identify, if possible, the true expansion process or at least to ascertain which expansion mode assumption appears to be better. In addition, from the standpoint of erosion considerations, it is highly desirable to know where the formation of moisture will begin.

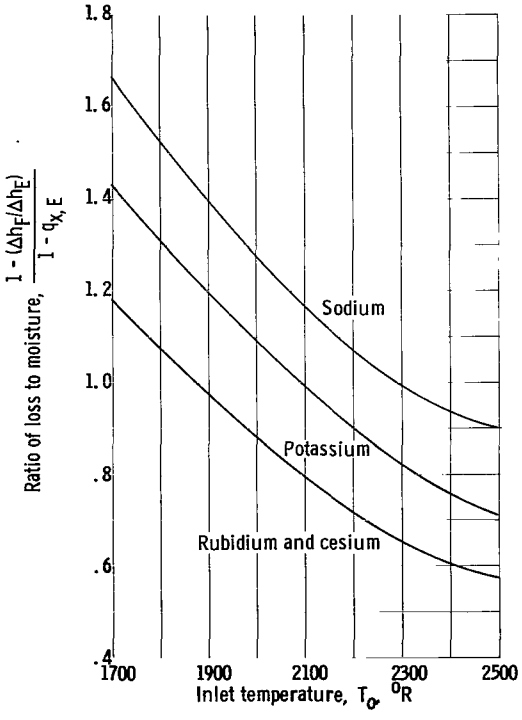

Figure 3. - Comparison of equilibrium energy loss and equilibrium moisture for supersaturated expansion.

NOZZLE CONDENSATION THEORY

The phenomenon of supersaturation was first reported in the literature about 80 years ago. Since that time, a vast amount of theoretical and experimental condensation studies have been made and reported. The intent of this study is not to review and discuss condensation theories but to apply existing theory to the case of metal vapors, especially the alkali-metal vapors being considered for use in space power systems. For a complete background of condensation studies excellent reviews and bibliographies are given in references 1, 3, and 4. The equations pertinent to this analysis will be presented but not derived in this section since the derivations can be found in the literature.

Condensation theory was successfully applied to flow in nozzles in reference 5, where it was shown that the condensation behavior of steam could be predicted surprisingly well from one-dimensional frictionless flow theory, perfect gas relations, liquid drop nucleation theory, and kinetic theory mass and energy transfer considerations. In view of the successful application of the nozzle-flow analysis of reference 5 to the case of steam, this analysis for metal vapors will be made in a similar manner. It is entirely possible, however, that the pertinent mechanisms associated with the condensation of metal vapors as they rapidly expand through a nozzle are not the same as for steam. This point will be subsequently discussed in more detail.

The basic assumptions of the analysis are: (1) flow is one-dimensional, frictionless, and adiabatic, (2) the perfect gas relations can be used for the vapor phase, (3) the liquid drop velocity is equal to the vapor velocity, and (4) the molecular specie content of the vapor, for purposes of calculating the bulk vapor properties, is frozen at its initial value. The pertinent system of differential flow equations is

Continuity:

$$\frac{1}{A}\frac{dA}{dx} + \frac{1}{\rho}\frac{d\rho}{dx} + \frac{1}{u}\frac{du}{dx} = 0 \tag{1}$$

Momentum:

$$u\frac{du}{dx} = -\frac{g}{\rho}\frac{dp}{dx} \tag{2}$$

Energy:

$$\frac{d}{dx}\left[\frac{u^2}{2gJ} + c_pT - (1 - q)\Delta h_V\right] = 0 \tag{3}$$

Neglecting the liquid volume and applying the perfect gas law yield

$$\rho = \frac{\rho_V}{q} = \frac{pM}{qRT} \tag{4}$$

Substituting equation (4) into equations (1) and (2) and rearranging equations (1) to (3) yield the desired form of the equations

$$\frac{du}{dx} = \frac{\frac{1}{q}\frac{dq}{dx} - \frac{1}{A}\frac{dA}{dx} - \frac{\Delta h_V \frac{dq}{dx}}{T\left[c_p - (1 - q)\frac{d(\Delta h_V)}{dT}\right]}}{\frac{1}{u} - \frac{Mu}{gqRT} + \frac{u}{gJT\left[c_p - (1 - q)\frac{d(\Delta h_V)}{dT}\right]}} \tag{5}$$

$$\frac{dp}{dx} = - \frac{pMu}{gqRT} \frac{du}{dx} \tag{6}$$

$$\frac{dT}{dx} = - \frac{\frac{u}{gJ} \frac{du}{dx} + \Delta h_V \frac{dq}{dx}}{c_p - (1 - q) \frac{d(\Delta h_V)}{dT}} \tag{7}$$

An additional equation is needed to describe the differential amount of condensation. On the basis of kinetic theory considerations, this can be expressed in a manner similar to that shown in reference 5, that is,

$$- \frac{dq}{dx} = \frac{4\pi\lambda\rho_V(T_s - T)}{wu} \int_{x_o}^{x} r^2_{x',x} I^*_{x'} A_{x'} \, dx' \tag{8}$$

where

$$r_{x',x} = r_{x'} + \int_{x'}^{x} \frac{\lambda\rho_V(T_s - T)}{\rho_l u} \, dx \tag{9}$$

and

$$\lambda = \frac{3R\sqrt{3RTg}}{8 \, \Delta h_V J M^{3/2}} \tag{10}$$

Equation (8) represents, for position x in the nozzle, the differential change in vapor quality due to the growth of all previously formed condensation nuclei. The term $r_{x',x}$ represents the radius at position x of a condensation nucleus formed at any position x' upstream of position x. Expressions for the rate of formation I^* of the condensation nuclei and the radius r^* of these nuclei will complete the necessary set of equations.

The liquid drop theory of nucleation has worked out well for predicting the experimental condensation behavior of a variety of vapors. Several equations, all basically of the same form, for predicting nucleation rate as a function of temperature, pressure, and fluid properties have been obtained by various investigators. One such equation, attributed to Frenkel, is presented in references 1 and 3 as

$$I^* = \frac{p^2 M}{N\rho_l (kT)^2} \sqrt{\frac{2\sigma g N}{\pi M}} \, e^{-4\pi\sigma r^{*2}/3kT} \tag{11}$$

This equation predicts the rate of formation of liquid drops of radius r^*, which are the condensation nuclei. The radius r^* is often called the critical radius since it is the radius of drops in equilibrium with a supersaturated vapor according to the Helmholtz equation (refs. 1, 3, and 5)

$$\ln \frac{p}{p_s} = \frac{2\sigma M}{\rho_l RTr} \tag{12}$$

For a vapor with pressure p and temperature T, $r = r^*$. A liquid droplet of radius $r < r^*$, as seen from equation (12), has an equilibrium pressure that is greater than the environmental pressure (which corresponds to r^*) and, consequently, this droplet will evaporate. A droplet of radius $r > r^*$, on the other hand, has an equilibrium pressure that is less than the environmental pressure, and this droplet will continue to grow. The droplet of radius r^*, consequently, is stable at its point of formation and will grow as the expansion continues. As far as this system is concerned, therefore,

$$r^* = \frac{2\sigma M}{\rho_l RT \ln \frac{p}{p_s}} \tag{12a}$$

Equations (4) to (11) and (12a) are the complete set of equations used for this analysis. Numerical techniques were used to solve these equations. An outline of the steps followed in the machine-computation procedure is presented in the appendix. The required fluid properties were obtained from references 2 and 6. The surface tensions at the temperatures of interest were obtained from equation (18) of reference 7, which is

$$\sigma = \sigma_{mp} \left(\frac{T_c - T}{T_c - T_{mp}} \right)^{1.2} \tag{13}$$

where σ_{mp}, T_c, and T_{mp} are from reference 6.

RESULTS OF ANALYSIS

As a first step in the analysis, the theoretical nucleation rates for the fluids of interest were examined in the hope of obtaining a preliminary clue to the condensation behavior of rapidly expanding metal vapors and possibly evolving a simplified method for predicting this behavior. After this preliminary nucleation rate analysis was completed, the nozzle-flow analysis was conducted. The fluids of primary interest were sodium, potassium, rubidium, cesium, and mercury. Nozzle inlet temperatures examined for the alkali metals ranged from 1700° to 2500° R, while those for mercury were in the range of 1200° to 1600°R.

Nucleation Rates

As seen from equations (11) and (12a), the nucleation rate for any given fluid depends only on the environmental temperature and pressure. For any con-

stant nucleation rate, therefore, the required supersaturation pressure ratio p/p_s becomes a function of temperature alone. The supersaturation pressure ratio is plotted against temperature at several constant nucleation rates in figure 4 for water, sodium, potassium, rubidium, cesium, and mercury. Examination of these nucleation rate curves, neglecting the other material shown in this figure for the time being, indicates the direction of the nucleation process as a function of temperature and fluid. The supersaturation pressure ratio required to yield any given nucleation rate is seen to decrease with increasing temperature; this indicates that nucleation occurs more readily at higher temperature levels. The curves for the alkali metals (figs. 4(b) to (e)) show that the nucleation rate curves lie closer to the saturation line ($p/p_s = 1$) as molecular weight increases (from sodium to potassium to rubidium to cesium). This indicates that nucleation occurs more readily for the higher molecular weight alkali metals. Since the indicated nucleation behavior of the alkali metals relative to each other depends to a large extent on the relative surface tension values, a degree of uncertainty must be associated with the indicated fluid effect. For mercury (fig. 4(f)), in the temperature range of interest, the supersaturation pressure ratio required for any given nucle-

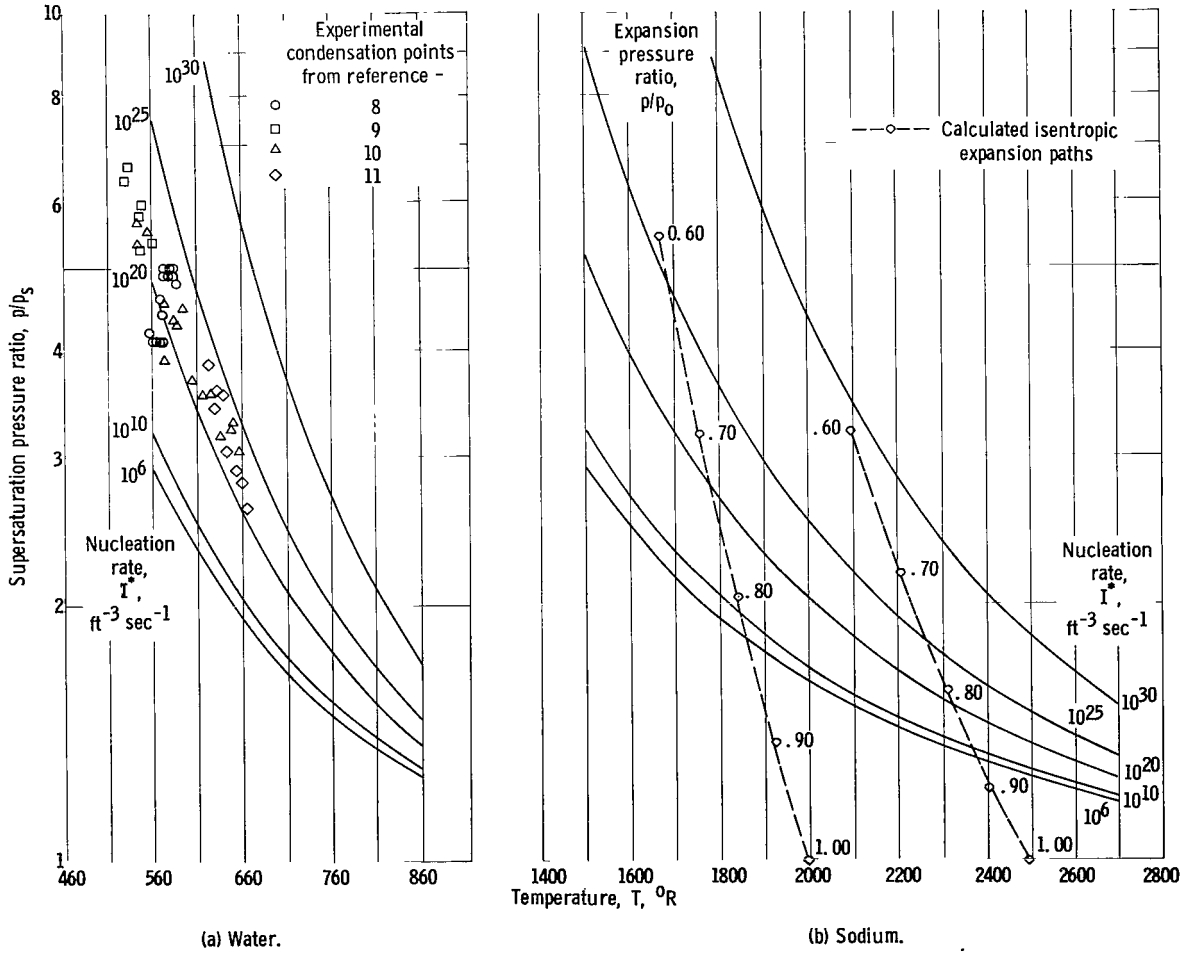

Figure 4. - Theoretical nucleation rate contours.

ation rate is about 1 to 3 orders of magnitude greater than those for water or the alkali metals at their temperatures of interest. This behavior can be attributed to the extremely high surface tension of mercury and implies that mercury nucleation does not occur very readily and high degrees of supersaturation may occur during a rapid expansion.

The most extensive experimental nozzle condensation studies that have been made are those for water; the theoretical nucleation rates for water are shown in figure 4(a). Condensation points obtained from nozzle experiments in references 8 to 11 are also shown in figure 4(a). The pressures corresponding to the onset of condensation were determined experimentally, while the temperatures were calculated by assuming an isentropic supersaturated expansion from the nozzle inlet to the condensation point. It is interesting to note that 37 of the 43 points lie between nucleation rates of 10^{20} and 10^{25}, while the remaining six points are slightly below a rate of 10^{20}. This seems to indicate that a significant nucleation rate required for the initiation of condensation may be in the region of $I^* = 10^{20} - 10^{25}$. If the condensation mechanism for the metal vapors is similar to that for steam, a significant nucleation rate for these metal vapors should be in the approximate order of magnitude region as that for steam. By using a condensation criterion of $I^* = 10^{20} - 10^{25}$ for the metal vapors, a simplified method for estimating the condensation point of the metal vapors can be evolved.

Since the coordinates of figure 4 are functions of only pressure and temperature, isentropic expansion paths can be plotted on the same figure. Isen-

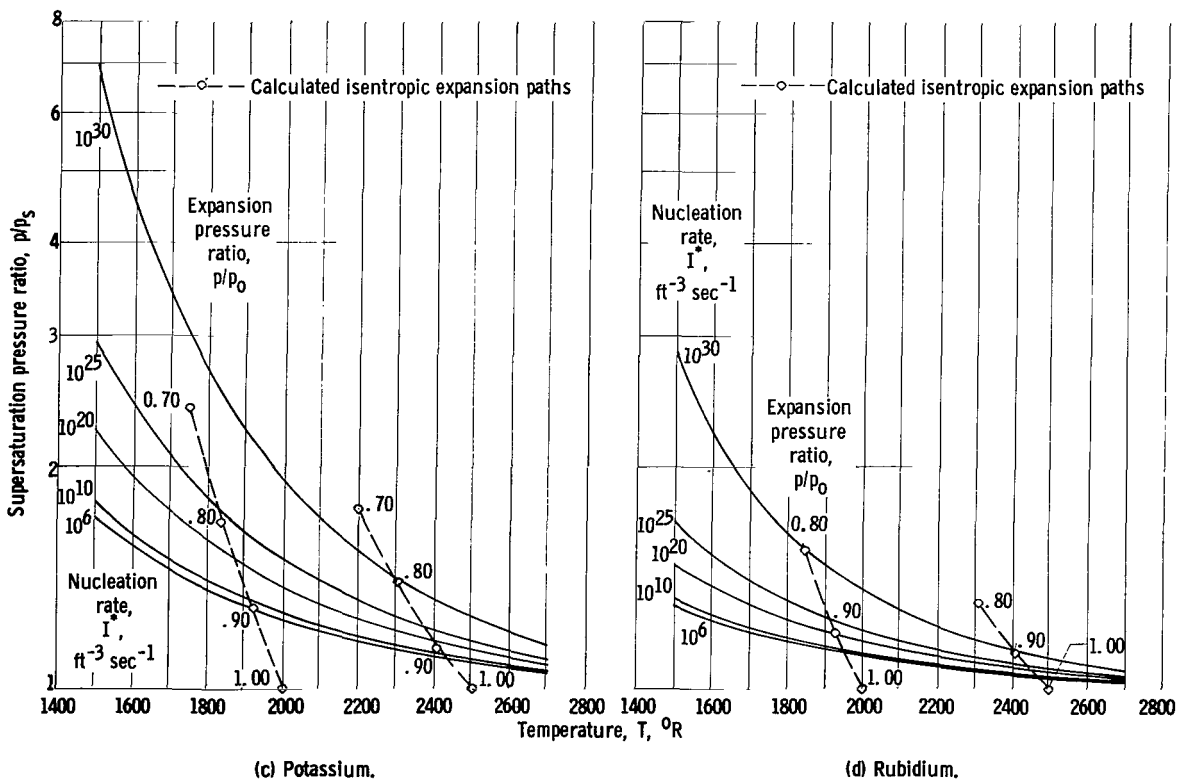

Figure 4. - Continued. Theoretical nucleation rate contours.

tropic expansion paths are shown in figures 4(b) to (f) for initially saturated vapors expanding from initial temperatures of 2000° and 2500° R for the alkali metals and 1200° and 1600° R for mercury. The points shown on each path represent the indicated expansion pressure ratios. With mercury (fig. 4(f)), the expansion proceeds well into the supersonic region ($p/p_o < 0.2 - 0.3$) without the occurrence of appreciable nucleation. The experimental results in reference 12 verify that extremely high supersaturation pressure ratios are achievable with mercury. In the case of the alkali metals (figs. 4(b) to (e)), the isentropic expansion paths cross the nucleation rate curves rather rapidly and reach values of $I^* = 10^{20} - 10^{25}$ while flow is still in the subsonic region ($p/p_o > 0.5$). The expansion pressure ratios corresponding to the bracketing values of the selected condensation criterion ($I^* = 10^{20} - 10^{25}$) are tabulated in table I (p. 14). An expansion pressure ratio corresponding to a point of initial condensation hereinafter will be termed condensation pressure ratio. A quantitative significance can now be given to the previously indicated temperature and fluid effects. Both increasing temperature and increasing molecular weight act to move the condensation point significantly toward the nozzle inlet. These results will be subsequently compared with the results of the nozzle-flow analysis in order to determine the accuracy of this estimation procedure relative to the more complex nozzle-flow analysis.

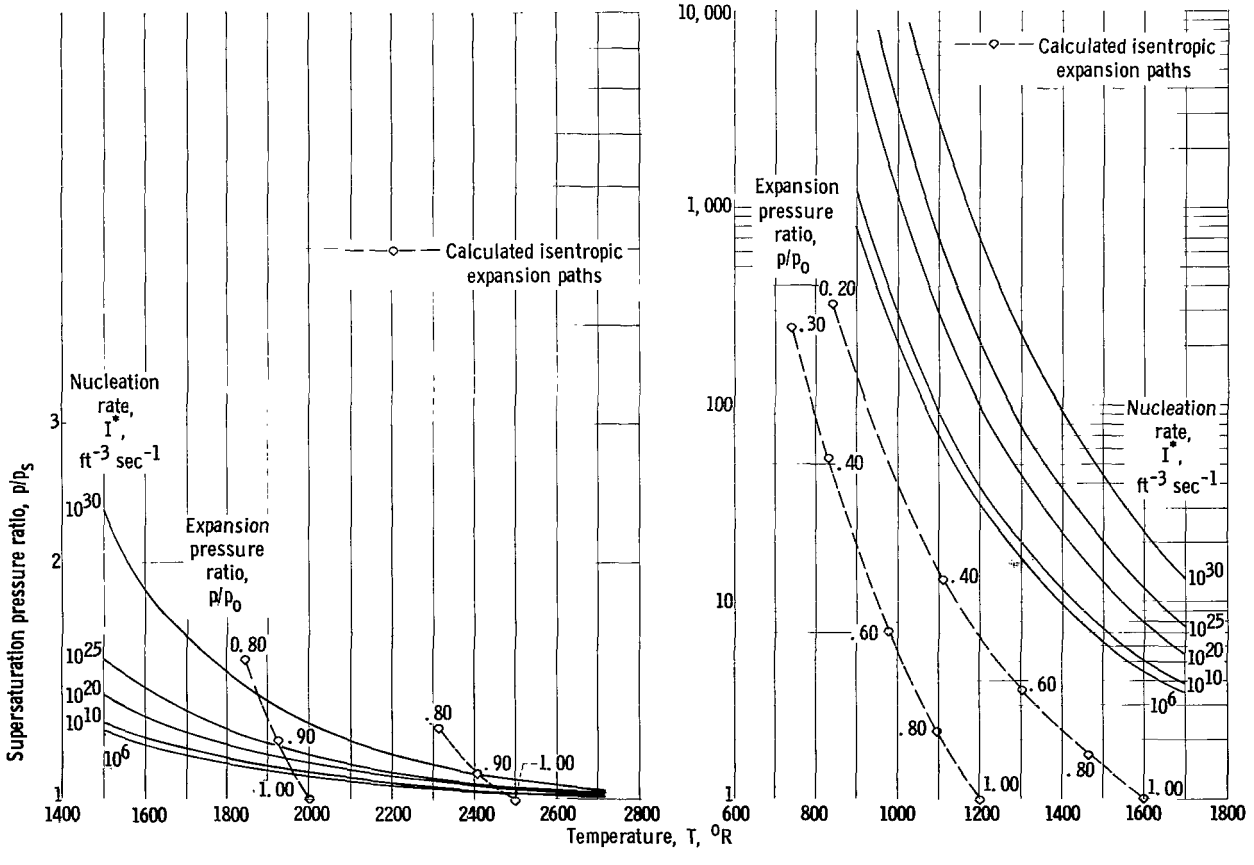

(e) Cesium. (f) Mercury.

Figure 4.. - Concluded. Theoretical nucleation rate contours.

TABLE I. - ESTIMATED CONDENSATION PRESSURE RATIOS

Fluid	Nozzle inlet temperature, °R	
	2000	2500
Sodium	0.62 to 0.73	0.76 to 0.82
Potassium	.79 to .84	.86 to .89
Rubidium	.88 to .90	.93 to .95
Cesium	.91 to .93	.94 to .96

Nozzle Flow

The nozzle-flow analysis method used in this study is similar to the analysis methods used in references 1 and 5, where these methods were shown to successfully predict the simultaneous expansion and condensation behavior of steam. For the purpose of checking the computation program, the analysis was applied to one of the experimental runs of reference 10. The results of this calculation are presented in figure 5 where the experimental and calculated pressure profiles and condensation points are compared. The nozzle-flow analysis predicts the behavior of steam quite well; the pressure profiles agree remarkably well, and the visually observed condensation front corresponds to the calculated condensation position.

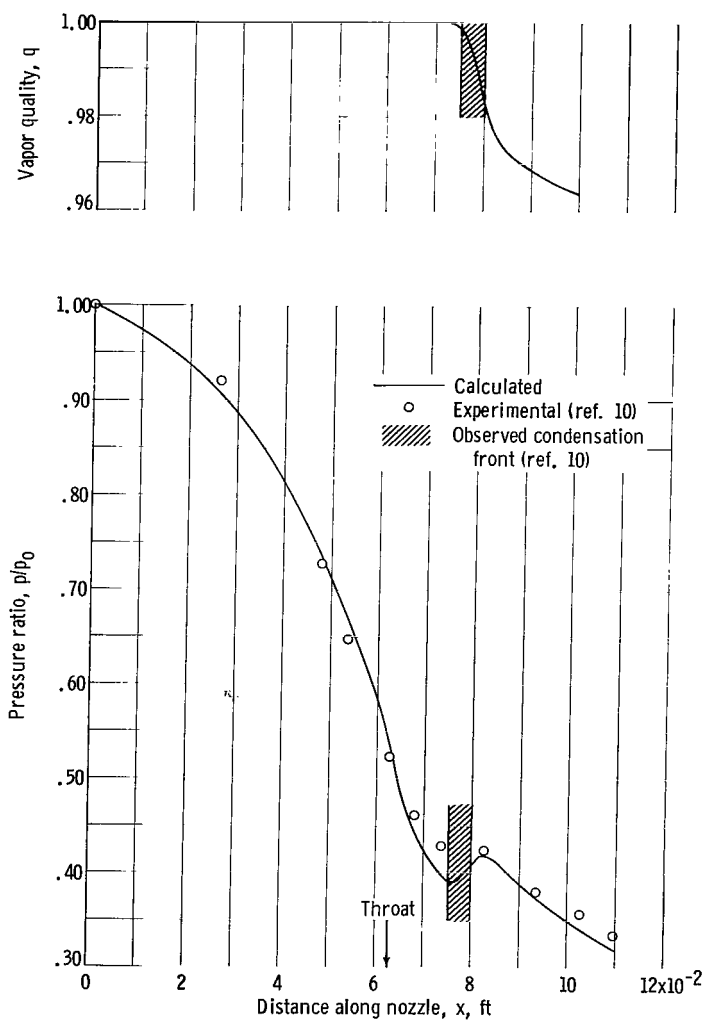

Figure 5. - Comparison of calculated and experimental expansion behavior for steam.

The nozzle-flow analysis was applied to the metal vapors. Mercury, as was indicated previously by nucleation rate considerations, was found to expand into the supersonic region to low pressure ratios ($p/p_o < 0.2$) without condensing, and the calculated expansion behavior corresponded to ideal gas behavior. Example results for an alkali-metal vapor expansion are presented in figure 6 where nozzle area ratio, expansion pressure ratio, temperature, vapor quality, and nucleation rate are plotted against axial distance for saturated potassium at 2100° R expanding through two nozzles. The two nozzles had equal lengths and equal inlet and exit (throat) diameters, but one had a conical flow passage, while the other had an elliptical flow passage in order to yield significantly different area ratios for the two cases. For the example conditions used in figure 6, condensation occurs upstream of the nozzle throat. As will be seen, nearly all the conditions of interest for the alkali metals result in conden-

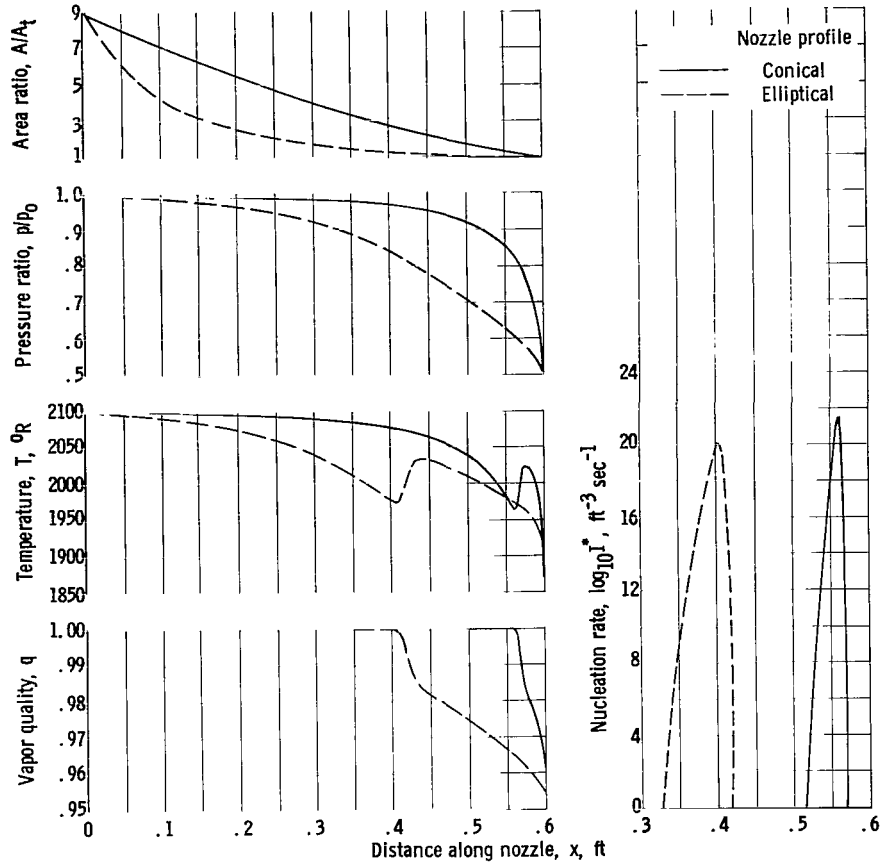

Figure 6. - Example of expansion characteristics of condensible vapor. Fluid, potassium; inlet temperature, 2100^0 R; inlet pressure, 43.9 pounds per square inch absolute (saturated).

sation in the subsonic flow region.

Subsonic condensation (fig. 6) causes very little pressure disturbance in the nozzle as opposed to supersonic condensation (fig. 5), which results in a definite rise in pressure. This pressure disturbance, because of its small magnitude, is not noticeable in figure 6. There can be, however, a significant temperature rise, which is about 60^o for the example case, because of the sudden release of the latent heat of vaporization. As will be subsequently shown, the magnitude of this temperature rise depends on the location of the initial condensation. The quality curves show that the initial condensate is rapidly formed as the vapor reverts from a supersaturated condition to a near-equilibrium condition. The nucleation rate increases quite rapidly (many orders of magnitude) just prior to condensation and then decreases again as soon as moisture is formed. The maximum nucleation rate, which occurs at the point of condensation, is seen to be in the region ($I^* = 10^{20} - 10^{25}$) previously selected as the condensation criterion for the simplified condensation point estimation procedure. In fact, over the range of nozzle inlet temperatures (1700^o to 2700^o R) investigated for the alkali metals, the nucleation rates at the condensation points were all in the range of $I^* = 10^{19} - 10^{26}$.

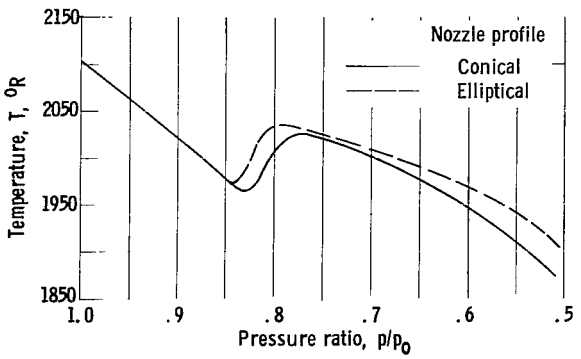

Figure 7. - Example temperature-pressure ratio characteristics for expansion of condensible vapor. Fluid, potassium; inlet temperature, 2100° R; inlet pressure, 43.9 pounds per square inch absolute (saturated).

The shape of the nozzle-area-ratio profile (fig. 6) affects the location of the initial condensation through its effect on the rate of expansion. The condensation pressure ratios, however, are almost the same for both nozzles. In fact, plots of temperature against pressure ratio for the two nozzles (fig. 7) are quite similar despite the significantly different area-ratio profiles (see fig. 6). In order to present the results of the nozzle analysis in a manner that is not significantly affected by the nozzle-area-ratio profile, the results will be presented as temperature plotted against expansion pressure ratio. The location of the condensation point can then be established in terms of the condensation pressure ratio, and this location will be approximately valid over a wide range of nozzles.

The effects of temperature and fluid on the expansion and condensation behavior of the alkali-metal vapors are presented in figure 8 where temperature

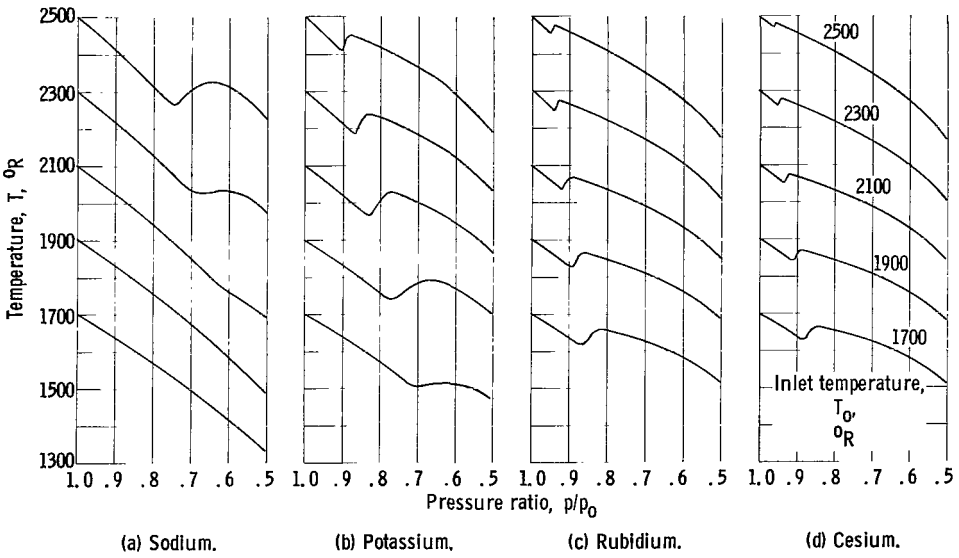

Figure 8. - Effect of temperature and fluid on expansion and condensation behavior of initially saturated alkali-metal vapors.

is plotted against expansion pressure ratio for initially saturated vapors of sodium, potassium, rubidium, and cesium expanding from several temperatures in the range of 1700° to 2500° R. Condensation is seen to occur upstream of the nozzle throat (subsonic region) for all cases shown in figure 8 except for sodium at inlet temperatures of 1700° and 1900° R. The study showed condensation to occur downstream of the nozzle throat (supersonic region) for sodium at

nozzle inlet temperatures below about 1950° R. The condensation points obtained from figure 8 are summarized in figure 9, where the condensation pressure ratio is plotted against the nozzle inlet temperature for the four alkali metals. Increasing nozzle inlet temperature results in the condensation point moving toward the nozzle inlet. An increase in nozzle inlet temperature from 1700° to 2700° R results in the condensation pressure ratio increasing from <0.5 to 0.80 for sodium, 0.71 to 0.93 for potassium, 0.86 to 0.96 for rubidium, and 0.88 to 0.98 for cesium. The effect of fluid is seen to be quite significant, especially at the lower temperatures where cesium and rubidium condense readily at pressure ratios of about 0.9 while sodium expands through the nozzle throat in a dry condition.

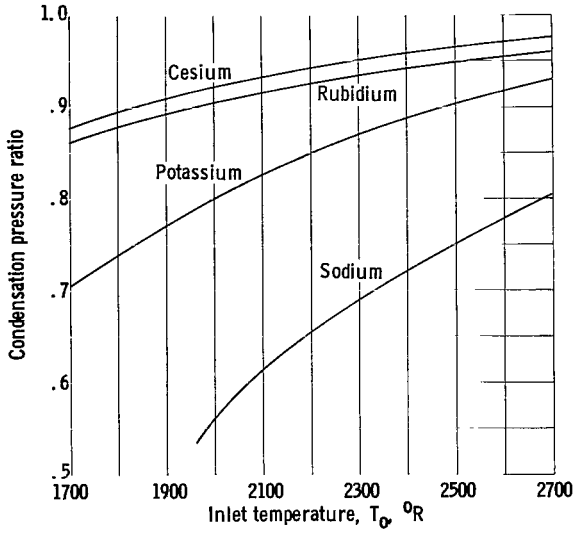

Figure 9. - Effect of inlet temperature and fluid on condensation pressure ratio.

The temperature rise due to the initial condensation reaches a maximum at a condensation pressure ratio of about 0.8 (fig. 8(b)). The amount of initial condensation and, consequently, the amount of heat released increases as the condensation pressure ratio decreases; the rate of expansion, however, is increasing and the temperature rise due to the released heat is being increasingly offset by the temperature drop associated with the expanding vapor. This interaction results in the observed maximum temperature rise. As the nozzle throat is approached, the rate of expansion becomes so rapid that there is no longer any temperature rise accompanying condensation. This can be seen from figure 8(a) at a nozzle inlet temperature of 2100° R; condensation merely causes a change in the rate of temperature decrease rather than a temperature increase.

The accuracy of the previously discussed condensation point estimation technique, which was based on the assumption of a nucleation rate criterion for condensation, can now be evaluated relative to the nozzle-flow analysis. A comparison of the previously tabulated values (table I, p. 14) for the estimated condensation pressure ratios with the calculated results presented in figure 9 shows that the calculated pressure ratios, in general, fall either within or very close to the estimated pressure ratio range. In the 2000° to 2500° R range of nozzle inlet temperatures, only for sodium does the calculated condensation pressure ratio differ by more than ±0.01 from the limiting values of the estimated pressure ratio range. The difference between the calculated and estimated values for sodium decrease from 0.06 at 2000° R to 0.01 at 2500° R. Since this estimation procedure is much simpler and much less time consuming than the nozzle-flow analysis, it can be very useful for preliminary calculations and for cases where approximate answers are satisfactory.

Since the condensation process depends on nucleation and growth rates, it

must depend to some degree on expansion time. The effect of expansion time on condensation is shown for an example case in figure 10 where temperature is plotted against pressure ratio for several nozzles with equal inlet and exit (throat) diameters but with lengths varying over a 10-to-1 range. A longer nozzle is seen to result in an increase in condensation pressure ratio. Even for a tenfold increase in length, however, the increase in condensation pressure ratio is only from 0.81 to 0.85. The effect of nozzle length and, consequently, expansion time on condensation pressure ratio, therefore, is quite small.

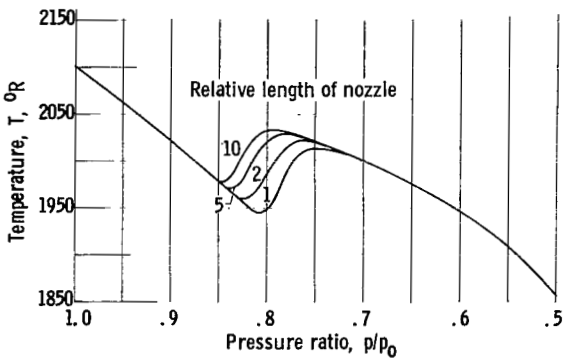

Figure 10. - Effect of expansion time on expansion and condensation behavior. Fluid, potassium; inlet temperature, 2100° R; inlet pressure, 43.9 pounds per square inch absolute (saturated).

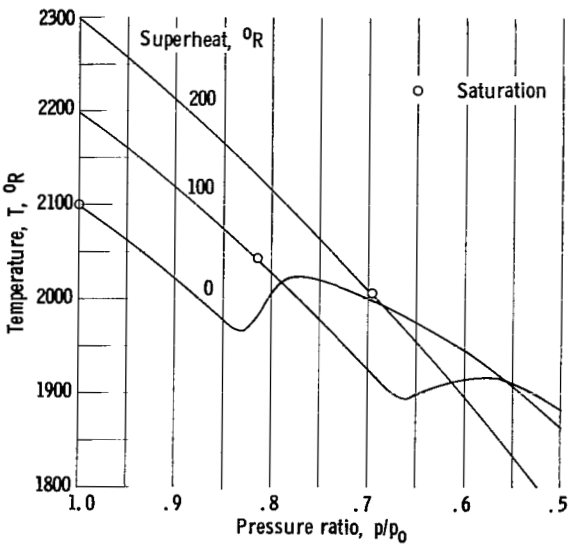

Figure 11. - Effect of superheat on expansion and condensation behavior. Fluid, potassium; inlet pressure, 43.9 pounds per square inch absolute; saturation temperature, 2100° R.

One possible method for delaying condensation, if this is desirable, is the use of superheated inlet vapors. The effect of superheat on condensation is shown in figure 11 where temperature is plotted against pressure ratio for an example case of a vapor both saturated and superheated 100° and 200° R. For the example shown, a superheat of 100° R shifts the condensation pressure ratio from 0.83 to 0.66, while a superheat of 200° R results in a dry expansion to the nozzle throat ($p/p_o \cong 0.5$). The use of superheat, consequently, can result in a significant reduction in condensation pressure ratio.

As mentioned previously, alkali-metal vapor turbine design and analysis procedures, for lack of knowledge concerning the true expansion mode, are based on either the purely frozen or the purely equilibrium mode of expansion. The foregoing discussion has shown that, for most of the cases of interest, supersaturation will occur up to a certain point and then condensation will commence. The following simplified analysis procedure for flow in nozzles is, therefore, suggested.

(1) Assume a frozen expansion from the nozzle inlet to the condensation point. A reasonable approximation for the condensation pressure ratio can be obtained from the proposed estimation technique.

(2) Assume an instantaneous step reversion to equilibrium. The associated

changes in temperature, pressure, and velocity are determined from diabatic flow considerations with a heat addition equal to the amount of latent heat released upon reversion.

(3) Assume an equilibrium expansion from this point to the nozzle exit. An approximation of the true expansion behavior can be obtained in this manner.

LIMITATIONS OF ANALYSIS

The uncertainties associated with this analysis warrant emphasis. The previously listed basic assumptions, with the exception of the frozen specie assumption, should introduce no significant source of error. The assumption of a frozen molecular species content for purposes of calculating the bulk vapor properties results from a lack of knowledge concerning the kinetic behavior of the bulk vapor-phase dimerization reaction, and will yield erroneous results only if this reaction does take place in the nozzle. Since the direction of the reaction would be from dimer to monomer, heat would be absorbed and condensation would tend to occur sooner than predicted on the basis of the frozen assumption.

The mechanisms assumed for nuclei formation and droplet growth may not be the correct mechanisms for the case of metal vapors although they seemed to work quite well for steam. The nucleation and growth equations are actually steady-state equations. If the period of time required to reach the steady-state condition is sufficiently small with respect to the distance traversed in the nozzle, then a quasi-steady-state treatment of the problem is reasonable. On the other hand, if the expansion is so rapid that steady-state conditions cannot be achieved at each point in the nozzle, the assumed equations will not predict the actual behavior and condensation will occur later than predicted by the steady-state equations. Another uncertainty stems from the interatomic attractive force associated with atoms of low electronegativity, such as the alkali metals. If a significant attractive force exists between the atoms, the entire growth process and, consequently, condensation will occur more rapidly than predicted by kinetic theory heat and mass transfer considerations.

Another area of potential inaccuracy for this analysis is associated with the values used for the surface tension of the fluids. The nucleation rate equation is completely dominated by the value of the exponential term. As can be seen from combining equations (11) and (12a), surface tension to the third power appears in this exponent; a small error in surface tension, consequently, results in a significant error in the calculated nucleation rate. There are two basic sources of error associated with the values used for surface tension. The values of surface tension used for this analysis are those corresponding to a flat surface of liquid. Although it is recognized that surface tension becomes a function of drop radius for the small drop sizes involved in the nucleation process, the nature of this dependency is quite uncertain. Different approaches to the drop radius dependency problem yield completely opposite results (ref. 3). The second potential source of error is the available value for the flat film surface tension. The available surface tension values for the alkali metals are quite meager, of questionable accuracy, and mostly for

temperatures in the vicinity of the melting point, which is approximately 2000° lower than the temperature of interest. These available values, therefore, must be extrapolated over a wide span of temperature by some approximate extrapolation technique (e.g., eq. (13)) that depends upon a knowledge of the fluid critical temperature. According to reference 6, there is about a ±20 percent range of uncertainty associated with the available critical temperatures. As a result of these considerations, the accuracy of the utilized surface tension values is quite uncertain.

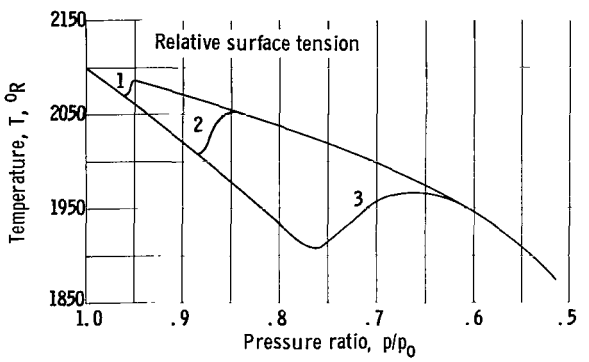

Figure 12. - Effect of surface tension on expansion and condensation behavior. Fluid, potassium; inlet temperature, 2100° R; inlet pressure, 43.9 pounds per square inch absolute (saturated).

In view of these surface tension considerations, the effect of varying surface tension on the location of the condensation point was investigated for an example case. Temperature is plotted against expansion pressure ratio in figure 12 for relative surface tension values of 1, 2, and 3. As seen from this figure, surface tension has a very significant effect on the condensation pressure ratio, which decreases with increasing surface tension. For a calculated condensation pressure ratio of 0.88, a ±50-percent uncertainty in surface tension could place the condensation pressure ratio anywhere between 0.96 and 0.76. The uncertainties inherent in the surface tension values used in this study, therefore, can significantly affect the position of the initial condensation and, for many cases, move the condensation point into or out of a nozzle.

SUMMARY OF RESULTS

This investigation was undertaken in order to gain some insight to the expansion and condensation behavior of metal vapors flowing through nozzles. The equilibrium and frozen modes of expansion were compared in order to determine the significance of the expansion mode assumption. A condensation analysis was then carried out in order to identify the true expansion mode. Nucleation rates were examined and condensation theory was applied to flow in nozzles. The nozzle-flow analysis used in this study can successfully predict the condensation behavior of steam during expansion; this analysis, however, may or may not be as successful for metal vapors depending upon the degree of similarity of the nuclei formation and droplet growth mechanisms for steam and metal vapors. Sodium, potassium, rubidium, cesium, and mercury were investigated at nozzle inlet temperatures of 1700° to 2500° R for the alkali metals and 1200° to 1600° R for mercury. The pertinent results of this study are summarized as follows:

1. A frozen expansion results in less ideal specific enthalpy drop and requires less flow area per unit weight flow than does an equilibrium expansion with the same pressure ratio. For a pressure ratio of 0.5, these enthalpy drop and area reductions are about 4 to 8 percent and 6 to 12 percent, respectively.

2. A simplified estimation procedure was evolved for predicting condensation pressure ratio on the basis of a nucleation rate criterion derived from steam considerations. Comparison with the more rigorous nozzle analysis showed that this estimation procedure can be used to predict a pressure ratio range that, in general, either includes or comes very close to the calculated condensation pressure ratio.

3. Mercury was found to expand to low pressure ratios (<0.2) without condensing. The alkali metals condense upstream of the nozzle throat (subsonic region) for all cases investigated except sodium at nozzle inlet temperatures below about 1950° R. A supersaturated expansion mode, therefore, appears to be the best assumption for an expansion process in a mercury system. For an alkali-metal system, supersaturation can be assumed up to the point of reversion, which can be estimated from the methods or results of this report, and equilibrium can then be assumed for the remainder of the nozzle.

4. Increasing either nozzle inlet temperature or molecular weight in the alkali-metal family resulted in the condensation point moving toward the nozzle inlet. An increase in nozzle inlet temperature from 1700° to 2700° R results in the condensation pressure ratio increasing from <0.5 to 0.80 for sodium, 0.71 to 0.93 for potassium, 0.86 to 0.96 for rubidium, and 0.88 to 0.98 for cesium.

5. Expansion time and superheat have small and large effects, respectively, on the location of the initial condensation. A tenfold increase in nozzle length for an example case resulted in only a small increase (0.81 to 0.85) in condensation pressure ratio. Superheating the inlet vapors 200° R for an example case resulted in a significant decrease (0.83 to about 0.5) in condensation pressure ratio.

6. The uncertainties inherent in the surface tension values used in this study can significantly affect the position of the initial condensation. For an example case considered in this study, a ±50-percent uncertainty in surface tension could place the condensation pressure ratio anywhere between 0.96 and 0.76.

Lewis Research Center
National Aeronautics and Space Administration
Cleveland, Ohio, June 25, 1964

APPENDIX - OUTLINE OF MACHINE-COMPUTATION

PROCEDURE FOR NOZZLE ANALYSIS

Since the analysis equations presented in the text are too complex for analytical solution, a stepwise numerical procedure was used to determine the temperature, pressure, velocity, and quality profiles for a nozzle. The nozzle was divided into a large number of small increments of length (dx was in the range of 0.001 to 0.0001 ft), and the calculation was made increment by increment from the nozzle entrance to the nozzle exit. The calculation procedure for one typical increment (going from x to x + dx) is outlined below.

Given:

(1) T, p, u, and q for all $0 \leq x' \leq x$

(2) All fluid properties (refs. 2 and 6) as a function of T and p

(3) Nozzle flow area A as a function of x

(4) $r^*_{x'}$ and $I^*_{x'}$ for $0 \leq x' \leq (x - dx)$

(5) Increment dx

Calculate:

(1) r^*_x from equation (12a)

(2) I^*_x from equation (11)

(3) $r_{x',x}$ for $0 \leq x' \leq x$ from equation (9)

(4) $\left(\frac{dq}{dx}\right)_x$ from equation (8)

(5) $\left(\frac{du}{dx}\right)_x$ from equation (5)

(6) $\left(\frac{dp}{dx}\right)_x$ from equation (6)

(7) $\left(\frac{dT}{dx}\right)_x$ from equation (7)

(8) $q_{x+dx} = q_x + \left(\frac{dq}{dx}\right)_x dx$

$$(9)\quad u_{x+dx} = u_x + \left(\frac{du}{dx}\right)_x dx$$

$$(10)\quad p_{x+dx} = p_x + \left(\frac{dp}{dx}\right)_x dx$$

$$(11)\quad T_{x+dx} = T_x + \left(\frac{dT}{dx}\right)_x dx$$

The selected increment was sufficiently small so that

$$\left(\frac{di}{dx}\right)_x \approx \frac{1}{2}\left[\left(\frac{di}{dx}\right)_x + \left(\frac{di}{dx}\right)_{x+dx}\right]$$

where $i = q, u, p,$ or T.

REFERENCES

1. Hill, P. G., Witting, H., and Demetri, E. P.: Condensation of Metal Vapors During Rapid Expansion. Jour. Heat Transfer (ASME Trans.), ser. C, vol. 85, no. 4, Nov. 1963, pp. 303-314; discussion, pp. 314-316.

2. Meisl, C. J., and Shapiro, A.: Thermodynamic Properties of Alkali Metal Vapors and Mercury. Rep. R60FPD358-A, General Electric Co., Nov. 9, 1960.

3. Stever, H. Guyford: Condensation Phenomena in High-Speed Flows. High-Speed Aerodynamics and Jet Prop., vol. III, Princeton Univ. Press, 1958, pp. 526-573.

4. Courtney, Welby G.: Recent Advances in Condensation and Evaporation. ARS Jour., vol. 31, no. 6, June 1961, pp. 751-756.

5. Oswatitsch, K. (M. Flint, trans.): Condensation Phenomena in Supersonic Nozzles. Z.a.M.M., vol. 22, no. 1, Feb. 1942, pp. 1-14.

6. Weatherford, W. D., Jr., Tyler, John C., and Ku, P. M.: Properties of Inorganic Energy-Conversion and Heat-Transfer Fluids for Space Applications. TR 61-96, WADD, Nov. 1961.

7. Gambill, Wallace R.: Surface and Interfacial Tensions. Chem. Eng., vol. 65, no. 9, May 5, 1958, pp. 143-146.

8. Binnie, A. M., and Woods, M. W.: The Pressure Distribution in a Convergent-Divergent Steam Nozzle. Proc. Inst. Mech. Eng., vol. 138, 1938, pp. 229-266.

9. Binnie, A. M., and Green, J. R.: An Electrical Detector of Condensation in High-Velocity Steam. Proc. Roy Soc. (London), ser. A, vol. 181, no. 985, Dec. 31, 1942, pp. 134-154.

10. Yellott, John I., Jr.: Supersaturated Steam. Trans. ASME, vol. 56, no. 6, June 1934, pp. 411-427; discussion, pp. 427-430.

11. Rettaliata, J. T.: Undercooling in Steam Nozzles. Trans. ASME, vol. 58, no. 8, Nov. 1936, pp. 599-605.

12. Kearton, W. J.: Some Experiments on the Flow of Mercury Vapour Through Nozzles. Proc. Inst. Mech. Eng., Dec. 1929, pp. 993-1025.

NASA-Langley, 1964 E-2482

"The aeronautical and space activities of the United States shall be conducted so as to contribute . . . to the expansion of human knowledge of phenomena in the atmosphere and space. The Administration shall provide for the widest practicable and appropriate dissemination of information concerning its activities and the results thereof."

—NATIONAL AERONAUTICS AND SPACE ACT OF 1958

NASA SCIENTIFIC AND TECHNICAL PUBLICATIONS

TECHNICAL REPORTS: Scientific and technical information considered important, complete, and a lasting contribution to existing knowledge.

TECHNICAL NOTES: Information less broad in scope but nevertheless of importance as a contribution to existing knowledge.

TECHNICAL MEMORANDUMS: Information receiving limited distribution because of preliminary data, security classification, or other reasons.

CONTRACTOR REPORTS: Technical information generated in connection with a NASA contract or grant and released under NASA auspices.

TECHNICAL TRANSLATIONS: Information published in a foreign language considered to merit NASA distribution in English.

TECHNICAL REPRINTS: Information derived from NASA activities and initially published in the form of journal articles.

SPECIAL PUBLICATIONS: Information derived from or of value to NASA activities but not necessarily reporting the results of individual NASA-programmed scientific efforts. Publications include conference proceedings, monographs, data compilations, handbooks, sourcebooks, and special bibliographies.

Details on the availability of these publications may be obtained from:

SCIENTIFIC AND TECHNICAL INFORMATION DIVISION

NATIONAL AERONAUTICS AND SPACE ADMINISTRATION

Washington, D.C. 20546